Rev. Adv. Mater. Sci. 52 (2017) 54-60

MAIN PATTERNS OF LATTICE FRAGMENTATION IN COPPER PROCESSED BY DYNAMIC EQUAL-CHANNEL ANGULAR PRESSING

V.V. Rybin[1,2], N.Yu. Zolotorevsky[1,2], E.A. Ushanova[2,3], S.N. Sergeev[4], A.N. Matvienko[1,2], I.V. Khomskaya[5] and D.N. Abdullina[5]

[1]Institute of Applied Mathematics and Mechanics, Peter the Great Polytechnic University, St-Petersburg 195251, Russia
[2]Mechanical Engineering Research Institute of the Russian Academy of Sciences, Nizhnii Novgorod 603024, Russia
[3]Central Research Institute of Structural Materials ''Prometey'', St-Petersburg 191015, Russia
[4]Institute of Superplasticity Problems of Russian Academy of Sciences, Ufa, S.Khalturina str. 39, Russia
[5]M.N. Miheev Institute of Metal Physics, Ural Branch, Russian Academy of Sciences, Ekaterinburg, S.Kovalevskaya str. 18, 620108, Russia

Received: July 15, 2017

Abstract. EBSD study of copper microstructure fragmentation under condition of high-speed deformation by dynamic channel angular pressing (DCAP) is presented. It has been shown that, in addition to regular fragmentation, extensive deformation twinning occurs during single DCAP pass. A local analysis of the misorientation evolution at individual twin boundaries during plastic deformation was conducted. Based on this analysis, the relationship between the deviation from exact twin misorientation and the strain, at which the twin has been nucleated, is suggested. The deformation twins are shown to appear mostly at a final stage of deformation, though the twinning seems to occur over whole pass of DCAP.

1. INTRODUCTION

It is well known that normal polycrystals may be changed into materials with an ultrafine-grained structure under large degrees of plastic deformation [1,2]. The cause of this transformation is a fragmentation of original grains. Namely, the grains loose their orientation uniformity and gradually subdivide to small regions (fragments) disorientated by angles higher than $\theta_0 \approx$ 1-2° [3-6]. The fragment misorientation (θ) and size (d) distributions obey certain statistical laws, whereas their average values θ_a and d_a correlate with the degree of macroscopic deformation [7]. At that, $\theta_a(\varepsilon)$ increases while $d_a(\varepsilon)$ decreases with increasing strain approaching saturated level about $d_0 \approx 0.2$–0.3 μm.

The rates of $\theta_a(\varepsilon)$ and $d_a(\varepsilon)$ changing are controlled by specific mechanisms of fragments formation. Among these mechanisms are (1) nucleation and subsequent development of terminating deformation-induced boundaries (DIBs), which appear predominantly near the boundaries of original grains [3,8,9]; (2) deformation-induced faceting of original grain and twin boundaries [10]; (3) fragmentation of deformation twins if the latter emerge [11]; (4) dynamic recrystallization in the fragmented structure [12]. Partial contributions of the mechanisms indicated above may vary within a wide range, since their appearance dependents on the type of crystal lattice, the stalking fault energy as well as the deformation scheme, temperature and rate. First these mecha-

Corresponding author: N.Yu. Zolotorevsky, e-mail: zolotorevsky@phmf.spbstu.ru

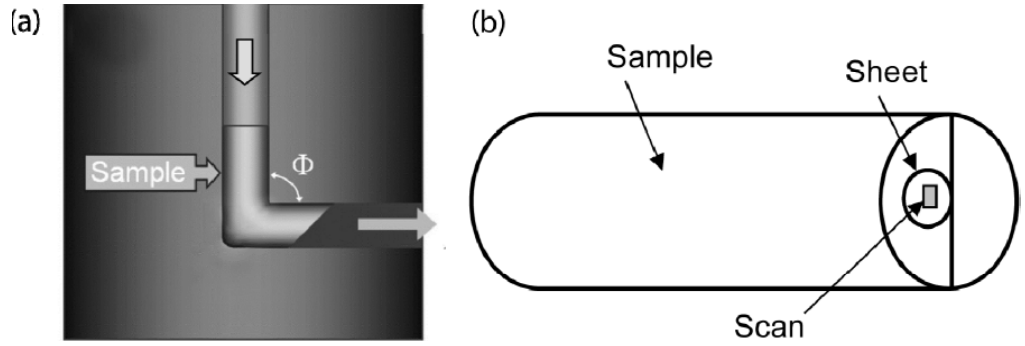

Fig. 1. Scheme of DCAP experiment (a) and location of examined area on the transverse section (b).

nisms and their partial contributions have been studied in detail with using methods of transmission and scanning microscopy by the example of fragmented structure of a plastic stream, which is formed under explosive welding of copper plates [10,11]. It turned out that surprisingly large amount (more than 25%) of the fragment boundaries are inherently twin boundaries, though their misorientations are highly deviated from the original twin one due to a plastic deformation. This observation can reasonably be associated with large strains ε and extremely high strain rates $\dot{\varepsilon}$ estimated to be

$$\varepsilon \sim 1-2;\ 10^5 < \dot{\varepsilon} < 10^6 c^{-1} \qquad (1)$$

in the plastic stream [13] . Actually, such strain rates are known to stimulate deformation twinning (DT) in technically pure copper [14,15]. However, systematic investigation of this matter is rather embarrassing on such an exotic and structurally inhomogeneous object as the plastic stream. To do this, it is necessary to examine a fragmented structure formed in a macroscopic sample under strain and strain rate conditions similar to that indicated above but with the deformation proceeding sufficiently uniformly over a specimen. The purpose of the present work was to perform such an investigation using dynamic channel angular pressing (DCAP) [16-19], a high-speed variant of the equal channel angular pressing (ECAP) [1] allowing above deformation conditions to be fulfilled.

2. EXPERIMENTAL

The experiment was conducted using technical copper (99.8%). A cylindrical sample was annealed initially at 450°C and then deformed by 1 pass of DCAP at room temperature [16]. The sample was 65 mm in length and 16 mm in diameter. The die had two channels of 16 and 14 mm in diameter intersecting at an angle Φ = 90° with zero inner radius of curvature and the outer radius of curvature equal to the radius of entrance channel (Fig. 1a). The sample was accelerated with a special gun under the action of gun-powder gases up to the rate of 230 m s^{-1} and directed it into the die. The strain rate was 10^5 s^{-1}, the time of deformation was 500 μs, and the pressure on a sample did not exceed 1.5 GPa [16]. The shear strain accumulated in a single pass of DCAP was estimates as 1.15 on the base of results obtained earlier for ECAP [1,5].

A thin circular sheet having radius of 3 mm was sliced perpendicular to the pressing direction from the region adjoining to the sample axis as shown in Fig. 1b. The sheet was then ground mechanically and finally electropolished. Two areas of 25*25 μm^2 (scans 1 and 2) located near centre of the sheet, i.e. within about 1.5 mm from the sample axis, have been investigated.

The microstructure was examined using an automated analysis of electron backscatter diffraction (EBSD) patterns with the help of the CHANNEL5 software package implemented in a TESCAN MIRA 3LMH scanning electron microscope with a field cathode. The orientation mapping of the initial and deformation microstructures was performed with the scanning steps of 2 μm and 50 nm, respectively. Subsequent processing of orientation data and the crystallographic analysis were carried out with MTEX software [20]. The minimum misorientation angle of 2° for identification of boundaries on orientation maps (the so called “tolerance angle”) was used to minimize the effect of orientation noise on the low-angle misorientation distributions [21]. Misorientation frequency distributions $\eta(\theta)$ were determined for the identified boundaries. Based on them, fractions of the boundaries belonging to various angular intervals were determined: (1) low angle dislocation boundaries, $2° \le \theta < 8°$, (2) medium angle boundaries, which structure varies from purely dislocation to grain-boundary one, $8° \le \theta < 15°$, and (3) high-angle boundaries, $15° \le \theta < 62.8°$. Among the high-angle boundaries, near-twin boundaries were distin-

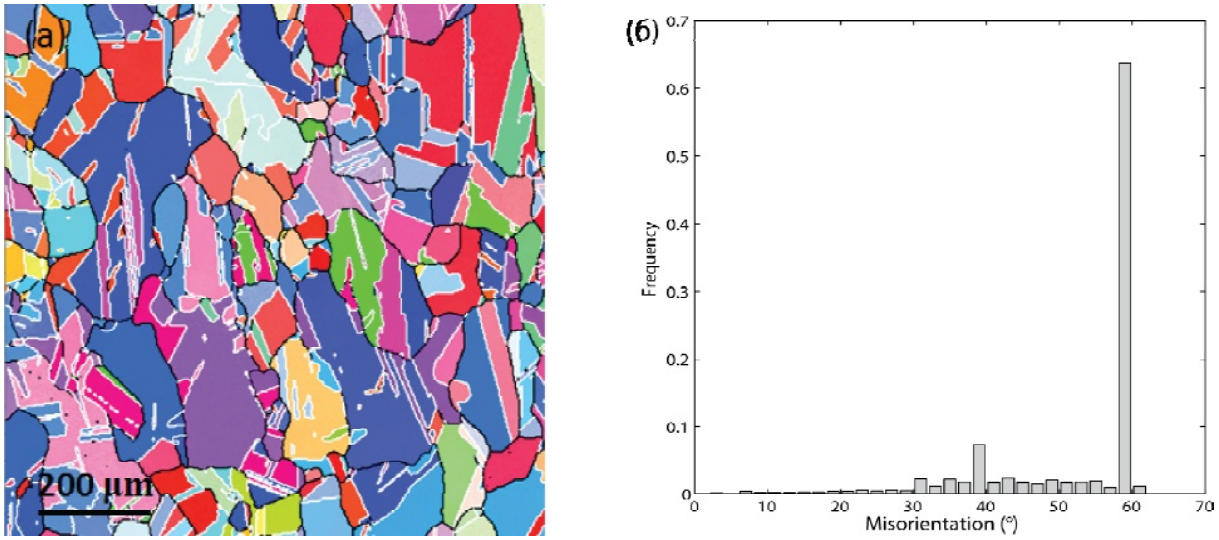

Fig. 2. Representative microstructure of recrystallized copper (inverse pole figure map of the bar longitudinal axis superimposed with the boundary map). Black lines: random grain boundaries; white lines: twin boundaries according to Brandon criterion.

guished. A closeness to the first-order twins ($\Sigma 3$) or second-order twins ($\Sigma 9$) was determined according to the Brandon criterion: angular deviation from the twin misorientation must be smaller than $\Delta\theta_c = 15°\sqrt{\Sigma}$. Besides the frequency distributions, the specific boundary length distributions $\lambda(\theta)$ were determined.

3. RESULTS AND DISCUSSION

3.1. Initial state

The microstructure shown in Fig. 2a is typical for cross section of a copper bar produced by plastic deformation and subsequent recrystallization. Slightly elongated grains are bounded by straight or smoothly curved boundaries. Considerable scattering of grain sizes within the range from several tens of micrometers to about 200 μm is observed. Multiple twin plates with a thickness of about 5 to 50 μm occur inside the grains. One can see in Fig. 2b that low and medium angle boundaries are almost absent in the recrystallized copper, approximately 98% of the boundaries are high-angle, the fractions of $\Sigma 3$ and $\Sigma 9$ boundaries are approximately 62% and 8%, respectively. Residual ~28% may be characterized as random grain boundaries (certain deviation from a random misorientation distribution [22] in the range 30°…40° may be associated with the occurrence of low-energy special boundaries with reciprocal densities of coincidence sites $5 \le \Sigma \le 29$ [23]). The crystallographic texture is not pronounced, that is evident from the coloring of orientation map in Fig. 2a.

3.2. Deformation state

The DCAP drastically changed the microstructure of copper, Fig. 3. A fragmentation of grain and annealing twin volumes, which earlier were oriented uniformly, occurred, while original grain boundaries lost their smoothness. Specific length of the boundaries increased significantly in all misorientation ranges (Fig. 4). Therewith, the length of low angle boundaries increased more than 3000 times, medium angle boundaries – more than 600 times, high angle boundaries – 18 times. The increase of specific length of near-twin boundaries can be approximately estimated from the histogram as ~ 8 times. Thereby, significant amount of twins appears during DCAP in additions to the annealing twins existed in the recrystallized copper.

3.2.1. Structure morphology

The sizes, shape and special arrangement of the fragments differ not only when going from one grain to the other, but even within a single grain. Two characteristic elements of the microstructure, referred to further as “packet” and “archipelago”, can be seen in Fig. 3.

The packet (marked by white dashed contour in Fig. 3a) is a cluster of several plate-like crystallites with the thickness of 5 to 10 μm extended in the same direction, oriented uniformly to within low angle misorientation but highly misoriented. Thinner plates with the thickness of about 1 μm are also observed sometimes, e.g. **A2** in Fig. 3a. In the maps of Fig. 3, the high angle random boundaries are

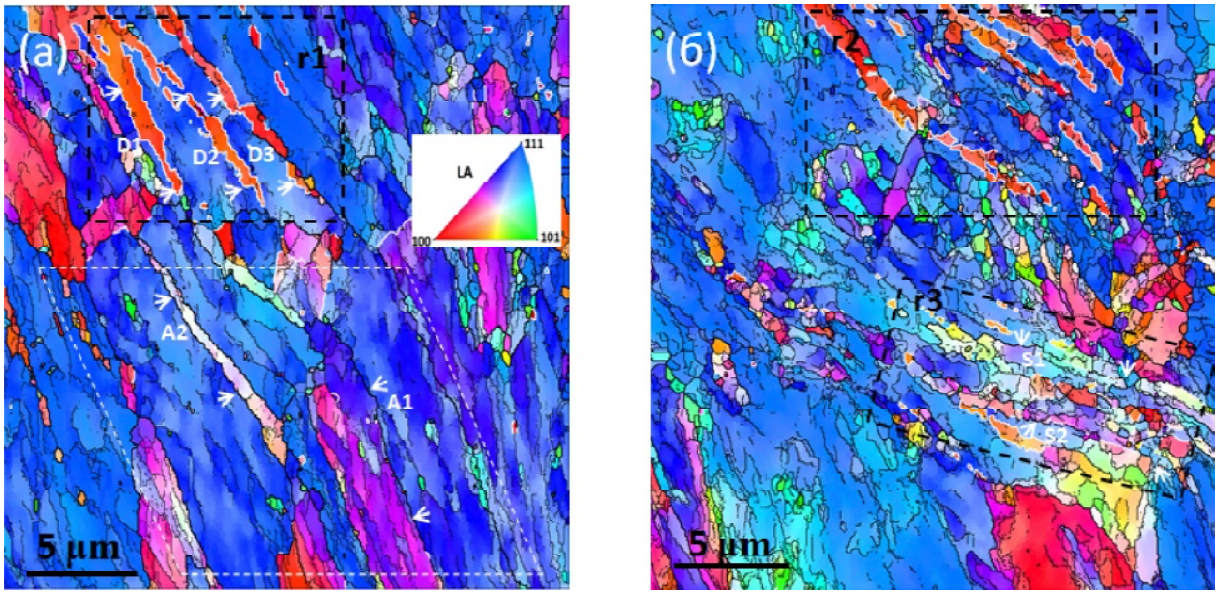

Fig. 3. Representative microstructures of copper deformed by DCAP (inverse pole figure map of the pressing direction superimposed with the boundary map: scan 1 (a) and scan 2 (b). Boundary coloring: black thin lines 2°< θ <15°; black thick lines: θ>15°; white lines: twin boundaries according to Brandon criterion. The regions of "archipelagos" are indicated by black dotted rectangles, the "packet" – by the white dashed parallelogram.

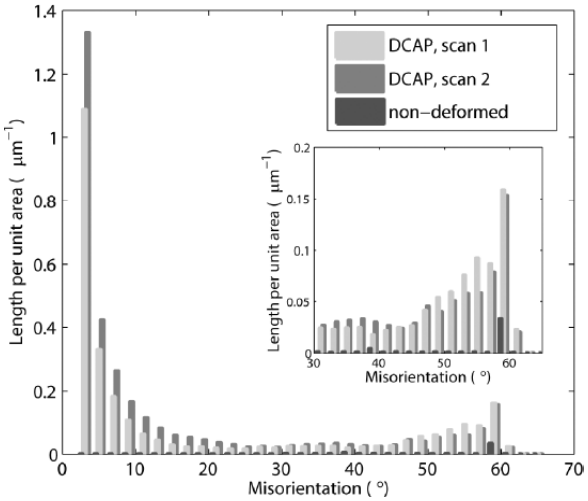

Fig. 4. Distributions of misorientation angles in recrystallized copper and after deformation by DCAP represented in terms of specific length of boundaries. Enlarged high-angle part of the histogram is inserted additionally.

black, while near-twin boundaries are white. Thus, the longitudinal boundaries in the packet are random judging from their misorientations; the latter deviate by more than $15/\sqrt{3} = 8.66$ from the twin one. At the same time, some transverse boundaries turn out to be near-twin.

Inside plates of the "packet" multiple unclosed DIBs occur. These boundaries extend themselves predominantly along the direction of plate elongation. Their length vary from about 2 to 5 μm, while the spacing between them – from 0.5 to 2 μm; the misorientations are mostly low angle.

The examples of structure peculiarities, which can be called symbolically as "archipelagos", are marked **r1**, **r2**, and **r3** in Fig. 3. Every archipelago manifest itself as a group of morphologically similar fragments. Often they take shape of chains being continuation of larger plate-like fragments extended along a certain direction. Multidirectional archipelagos may sometimes appear in a grain: e.g. **r2** and **r3** in Fig. 3b. The morphology of archipelagos suggests that their origin is related to the deformation twinning. This is also supported by the fact that the boundaries of fragments forming the archipelagos are mostly near-twin boundaries. Alternatively, near-twin boundaries are rarely found among the high-angle boundaries not included in the archipelagos.

3.2.2. Misorientation angle distributions

Fig. 5 represents the misorientation angle distributions obtained from the whole scans 1 and 2 shown in Fig. 3a and b in terms of frequencies. Additionally, one can see here the distributions obtained from the archipelago regions **r1**, **r2**, and **r3**.

In spite of clear morphological differences of the microstructures of scans 1 and 2, the corresponding misorientation distributions turned out to be quite

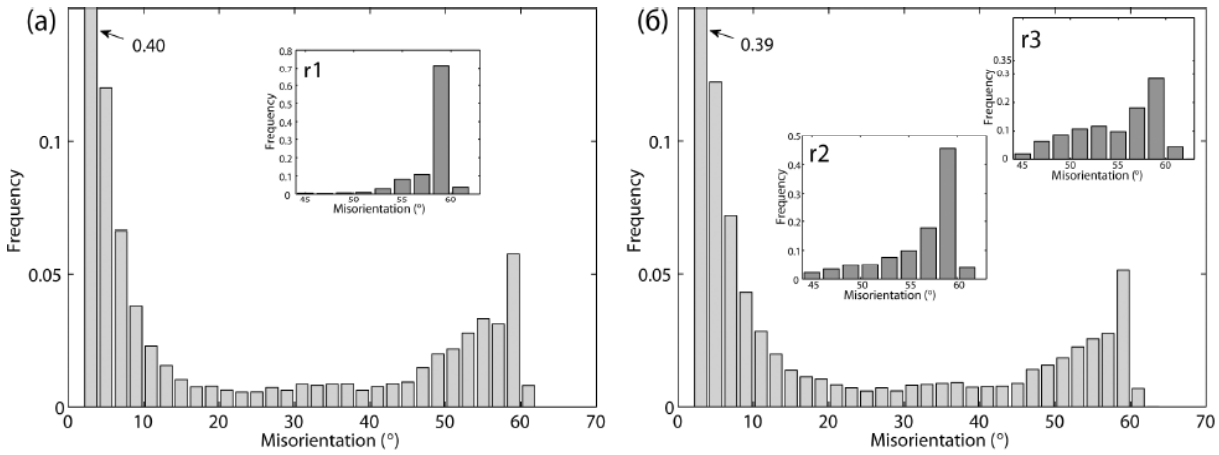

Fig. 5. Distributions of misorientation angles in copper after deformation by DCAP for scans 1 (a) and 2 (b). Additionally, the distributions obtained from the regions **r1**, **r2**, and **r3** are inserted**.**

similar. Three characteristic intervals on the histograms are: (1) $2°\leq\theta<16°$, (2) $16°\leq\theta<46°$ and (3) $46°\leq\theta<62°$. In the first interval, the relative fraction of boundaries $\eta(\theta)$ decreases steeply. In the second interval, variations of $\eta(\theta)$ are rather small. On the third interval, $\eta(\theta)$ increases steadily reaching its maximum at $\theta\in$58–60° and then decrease sharply down to zero. This specific appearance of the histogram indicates that during plastic deformation under conditions (1) the ensemble of DIBs in copper evolves as the result of interaction between lattice dislocations with the boundaries. During this evolution, some DIBs increase their misorientation while other – reduce it. At the same time, new boundaries progressively appear with misorientations near the ends of the range of allowable angles. At one end, these are low-angle DIBs, which appear as terminating boundaries with misorientations about 1–2° [3]. At the other end, these are deformation twin boundaries with misorientations of 60°. A compiling and solving of kinetic equation for determination of a DIB misorientation angle distribution function $\eta(\theta,\varepsilon)$ is not a purpose of this article. It is clear, however, that characteristic spreading will be developed on the misorientation histogram near θ = 2° and 60°, Fig. 5. Also it is clear that a height of these peaks and the shape of the spreading are determined by the crystal geometry and intensity of local plastic deformation, as well as the mechanism of nucleation and subsequent evolution of the DIBs. The same relates to the DIB distributions in terms of the boundary length, Fig. 4.

The above qualitative reasons agree well with the data represented in Fig. 5. In this article, a high-angle part of distributions is of the most interest. Here it is considered concerning misorientations of fragments, which constitute archipelagos. Corresponding local regions **r1**, **r2**, and **r3** are chosen so that each of them presents one structural element of this type. A high-angle intervals for each archipelago are shown as the histograms inserted in Fig. 5a (**r1**) and 5b (**r2** and **r3**). These three distributions are similar in regard to a maximum at $\theta\in$58–60° and reduced frequencies within the interval $44°<\theta<58°$. Nevertheless, a height of the maximum and the rate of reduction of $\eta(\theta)$ turned out to be different for them. This can be associated partially with poor statistic of measurements. However, primary roots of these differences seem to be physical: different intensities of dislocation flow in the local regions of deformed grains and/or nonsimultaneity of the twin nucleation. In order to look into this question, additional examination was conducted, namely, local misorientations [24] along typical and sufficiently long boundaries relating to the "packets" and "archipelagos" were determined with a step ~1 μm.

3.3. Local misorientations across high-angle boundaries experienced deformation

Seven boundaries have been chosen for examination, Fig. 3. Two of them (A1 and A2) belong to the above considered "packet". As one can see in Fig. 3a, these boundaries are not near-twin ones. Next three boundaries (D1, D2, and D3) belong to the archipelago **r1,** which, judging from its morphology, seems to consist of several rather thin deformation twins being at an early stage of their fragmentation. At that, misorientations across them are very close to the twin misorientation. The last pair of bounda-

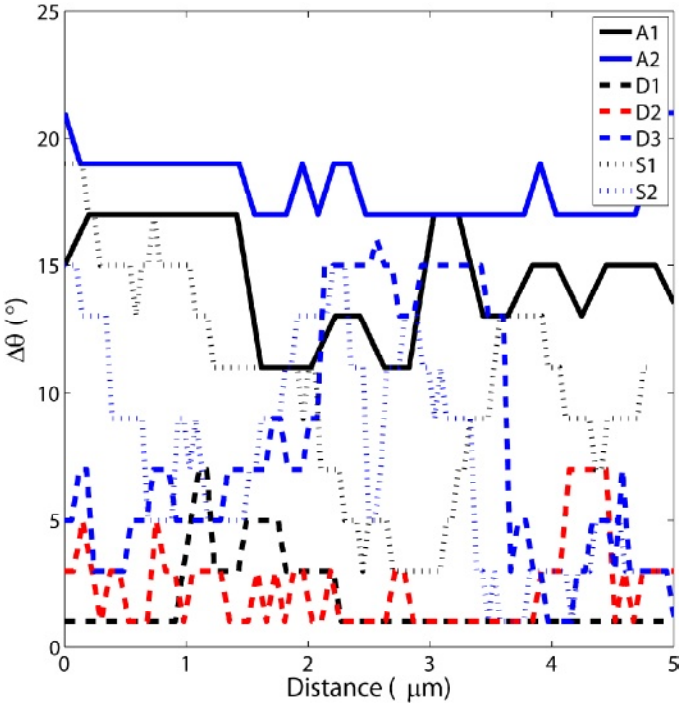

Fig. 6. Local angular deviation $\Delta\theta$ from the twin misorientation as function of the displacement along boundaries A1, A2, D1, D2, D3, S1 and S2 marked in Fig. 3.

ries (S1 and S2) belong to archipelago **r3,** which is composed of considerably more fragmented plates of deformation twins as well as a bundle of several dispersed fragments. As one can see from Fig. 3b, some of these fragments have boundaries close to the twin one.

The angular deviations $\Delta\theta$ from the twin misorientations determined on the base of measurements performed on these seven boundaries are shown in Fig. 6. They are represented as a function of displacement along a boundary; the start and the end points are shown by arrows in Fig. 3. Note that, in order to reduce orientation noise ~1–2° [21], measured values of $\Delta\theta$ are rounded to the nearest odd integers. In this case, residual oscillations of $\Delta\theta$ relates mostly to physical causes, such as a passage from one fragment adjoining to the boundary to another fragment or a heterogeneity of plastic deformation in the near-boundary region.

As for a mean level of deviation from the twin misorientation, it is natural to relate it with the value of plastic strain ε_T, at which the deformation twin has been nucleated. Assuming linear relationship between strain ε and the deviation $\Delta\theta$,

$$\Delta\theta(\varepsilon, \varepsilon_T) = \alpha(\varepsilon - \varepsilon_T). \quad (2)$$

One can estimate the coefficient α and then make an attempt to explain a role of twinning in the formation of different elements of the fragmented structure. Actually, as it is seen in Fig. 6, approximately 20-degree deviation is maximum for the structural state under consideration. This means that corresponding boundaries (A1 and A2) either took place in the initial recrystallized state being the annealing twins or nucleated as deformation twins in the beginning of the DCAP pass and subsequently developed forming the packet. Hence, the threshold strain $\varepsilon_T \approx 0$ for them. If total stain of a single DCAP pass $\varepsilon \approx 1$ then, with $\Delta\theta(1,0) \approx 20°$, $\alpha \approx 0.1\pi$ is obtained from Eq. (2). Knowing the coefficient α, one can now estimate the strain $\approx\varepsilon_T$, at which the structural elements of "archipelago" kind begin to form. Since $\Delta\theta \approx 1$–$3°$ for boundaries D1 and D2, one obtains $\varepsilon_T \approx 0.8$–$0.9$. Therefore, these deformation twins nucleate and form at the final stage of the deformation during DCAP pass. At the same time, such multiple twin plates seem to develop over whole pass of DCAP. This is evidenced from the data obtained for boundaries D3, S1, and S2, Fig. 6.

4. CONCLUSION

The mechanism of copper fragmentation under condition of extremely high-speed deformation have been studied by the example of DCAP, placing the emphasis on the twinning, which earlier was shown

to play significant role at explosive welding of copper plates [10,11]. The following main conclusions can be drawn based on the fragmented structure morphology and the misorientation distribution as well as on the variation of misorientations across individual boundaries of the twin origin.

1. Besides regular fragmentation of grain volumes, extensive deformation twinning occurs during single DCAP pass giving large contribution to the refinement of the copper microstructure.
2. The misorientations across boundaries of twin origin are significantly modified during plastic deformation, in particular, many of the annealing twin boundaries become arbitrary boundaries in terms of the Brandon criterion after single DCAP pass.
3. Based on the local analysis of misorientations across individual boundaries, it was shown that deformation twins appear mostly at a final stage of DCAP pass. At the same time, the twinning seems to occur over whole pass. The relationship between the deviation from exact twin misorientation and the strain, at which the deformation twin has been nucleated, is suggested.

ACKNOWLEDGMENTS

The authors appreciate financial support of the Russian Science Foundation, project No. 15-13-20030.

REFERENCES

[1] R.Z. Valiev and T.G. Langdon // *Progress in Materials Science* **51** (2006) 881.
[2] T.G. Langdon // *Acta Materialia* **61** (2013) 7035.
[3] V.V. Rybin, *Large plastic deformation and ductile failure of metals* (Metallurgiya, Moscow, 1986), In Russian.
[4] V.M. Segal, V.I. Reznikov, V.I. Kopylov, D.A. Pavlik, V.F. Malyshev, *Processes of metal structure formation* (Science and technology, Minsk, 1994), In Russian.
[5] R.R. Mulyukov, A.A. Nazarov and R.M. Imaev // *Proceedings of high schools. Physics.* **5** (2008) 47.
[6] D. Kuhlmann-Wilsdorf and N. Hansen // *Scripta metall. mater.* **25** (1991) 1557.
[7] D.A. Hughes and N. Hansen // *Acta mater.* **45** (1997) 3871.
[8].M. Seefeldt, L. Delannay, B. Peeters, E. Aernoudt and P. Van Houtte // *Acta Mater.* **49** (2001) 2129.
[9] A.E. Romanov and A.L. Kolesnikova // *Materials Science* **54** (2009) 740.
[10] V.V. Rybin, N.Yu. Zolotorevski and E.A. Ushanova // *Technical Physics* **59** (2014) 1819.
[11] V.V. Rybin, N.Yu. Zolotorevskii and E.A. Ushanova // *The Physics of Metals and Metallography* **116** (2015) 730.
[12] *F.J. Humphreys and M. Hatherly, Recrystallization and related annealing phenomena, second edition* (Elsevier, 2004).
[13] V.V. Rybin, E.A. Ushanova, S.I. Kuz'min and V.I. Lysak // *Tech. Phys. Lett.* **37** (2011) 1100.
[14] O. Johari and G. Thomas // *Acta Metall.* **12** (1964) 1153.
[15] Y. Xu, J. Zhang, Y. Bai and M. A. Meyers // *Metal.Mater.Trans.* **39A** (2008) 811.
[16] E.V. Shorokhov, I.N. Zhgilev and R.Z. Valiev // *RF Patent 2283717, Byull. Izobret.* **26** (2006) 64.
[17] V.I. Zel'dovich, E.V. Shorokhov, N.U. Frolova, I.N. Zhgilev, A.E. Kheifets, I.V. Khomskaya and V.M. Gundyrev // *Physics of Metals and Metallography* **105** (2008) 402.
[18] I.V. Khomskaya, E.V. Shorokhov ,V.I. Zel'dovich, A.E. Kheifets, N.Yu. Frolova, P.A.Nasonov, A.A. Ushakov and I.N. Zhgilev // *Physics of Metals and Metallography* **111** (2011) 612.
[19] G. Brodova, E.V. Shorokhov, A.N. Petrova, I.G. Shirinkina, I.V. Minaev, I.N. Zhgilev and A.V. Abramov // *Rev. Adv. Mater. Sci.* **25** (2010) 128.
[20] Florian Bachmann, Ralf Hielscher and Helmut Schaeben // *Ultramicroscopy* **111** (2011) 1720.
[21] A. Godfrey, O.V. Mishin and Q. Liu // *Materials Science and Technology* **22** (2006) 1263.
[22] J.K. Mackenzie // *Biometrika* **45** (1958) 229.
[23] W. Bollmann, *Crystal Defects and Crystalline Interfaces* (Springer Verlag, New York, 1970).
[24] N.Yu. Zolotorevsky, N.Yu. Ermakova, V.S. Sizova, E.A. Ushanova and V.V. Rybin // *J. Mater. Sci.* **52** (2017) 4172.